

# Neuromorphic Eye Tracking for Low-Latency Pupil Detection

Paul Hueber

*University of Manchester, UK*

paul.hueber@manchester.ac.uk

Luca Peres

*University of Manchester, UK*

luca.peres-2@manchester.ac.uk

Florian Pitters

*Viewpointsystem GmbH*

f.pitters@viewpointsystem.com

Alejandro Gloriani

*Viewpointsystem GmbH*

a.gloriani@viewpointsystem.com

Oliver Rhodes

*University of Manchester, UK*

oliver.rhodes@manchester.ac.uk

**Abstract**—Eye tracking for wearable systems demands low latency and milliwatt-level power, but conventional frame-based pipelines struggle with motion blur, high compute cost, and limited temporal resolution. Such capabilities are vital for enabling seamless and responsive interaction in emerging technologies like augmented reality (AR) and virtual reality (VR), where understanding user gaze is key to immersion and interface design. Neuromorphic sensors and spiking neural networks (SNNs) offer a promising alternative, yet existing SNN approaches are either too specialized or fall short of the performance of modern ANN architectures. This paper presents a neuromorphic version of top-performing event-based eye-tracking models, replacing their recurrent and attention modules with lightweight LIF layers and exploiting depth-wise separable convolutions to reduce model complexity. Our models obtain 3.7-4.1px mean error, approaching the accuracy of the application-specific neuromorphic system, Retina (3.24px), while reducing model size by 20 $\times$  and theoretical compute by 850 $\times$ , compared to the closest ANN variant of the proposed model. These efficient variants are projected to operate at an estimated 3.9-4.9 mW with 3 ms latency at 1 kHz. The present results indicate that high-performing event-based eye-tracking architectures can be redesigned as SNNs with substantial efficiency gains, while retaining accuracy suitable for real-time wearable deployment.

**Index Terms**—Eye Tracking, Neuromorphic, Spiking Neural Networks, Event-based Vision

## I. INTRODUCTION

Humans are unique among primates in having evolved eyes with a bright, uniformly white sclera, a feature that enhances the visibility of gaze direction and is fundamental to non-verbal communication [1,2]. The ability to discern gaze reveals focus and intent, a capability that modern eye-tracking technology seeks to automate and quantify. Eye tracking, the

process of measuring eye movements and positions, is thus a crucial method for understanding an individual's state and enabling interaction. It comprises critical metrics such as gaze direction, pupil diameter, and saccadic dynamics, which are essential for applications ranging from medical and psychological diagnostics [3,4] to human-computer interfaces in augmented and virtual reality (AR/VR) [5,6], robotics [7,8], and driver monitoring systems [9].

A core aspect of eye-tracking applications is pupil detection, the accurate and precise localization and tracking of the pupil within the visual field. This process enables the derivation of critical metrics such as gaze direction, blink rate, fixation duration, pupil diameter, and saccadic movement, forming the foundation for higher-level analyses. However, this task is exceptionally challenging due to the physiological characteristics of the human eye. As the fastest-moving organ in the human body, it can execute saccades of 15° amplitude with peak velocity of 500°s<sup>-1</sup> [10] with accelerations surpassing 24,000°s<sup>-2</sup> [11].

Conventional eye-tracking systems face fundamental limitations stemming from both their sensing and processing components. Frame-based cameras inherently struggle with motion blur during rapid saccadic movements [12], and face a critical trade-off between temporal resolution and energy efficiency. While high-speed cameras operating at kHz rates can mitigate latency issues, they do so at the cost of increasing power consumption [13], rendering them impractical for energy-constrained wearable systems [14]. Complementing these sensor limitations, conventional artificial neural networks (ANNs) introduce additional bottlenecks, as their computational intensity and sequential frame-processing paradigm struggle to maintain low-latency inference at high

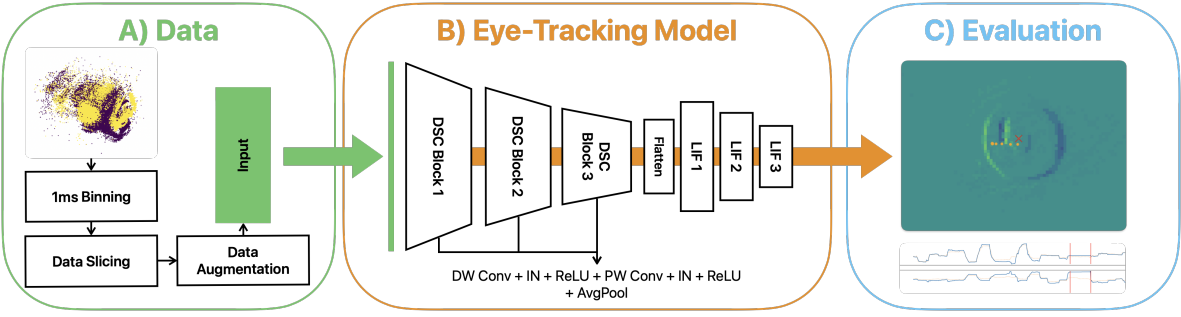


Figure 1. (A) Raw event streams are processed into 1 ms bins and sliced into 450 ms time windows for training and a continuous stream of 1 ms bins for evaluation and testing. The binned window is augmented using spatial and temporal transformations and CutOut. (B) Models are trained on the 450 ms sequences with a sliding window. (C) The best model from validation is evaluated in a continuous, online setting on the test set to simulate real-world deployment and report final performance.

throughput. This combination of hardware and algorithmic constraints typically limits practical systems to lower operational frequencies. For context, even demanding appreciations like foveated rendering require tracking updates at display refresh rates (90-120 Hz) with minimal latency to avoid user discomfort, a challenging target for power-constrained systems using conventional approaches.

Event-based cameras, also known as dynamic vision sensors (DVS), represent a paradigm shift in visual sensing with the potential to address limitations [15,16]. Unlike conventional cameras that capture full frames at fixed intervals, DVS can detect per-pixel brightness changes asynchronously, generating sparse event streams with microsecond temporal resolution, high dynamic range, and minimal motion blur [17,18]. This makes them particularly well-suited for pupil tracking, as they focus computational resources on dynamic eye movements while ignoring static regions [6,16].

Similarly, spiking neural networks (SNNs) provide a biologically-inspired processing framework that aligns well with the characteristics of event-based sensing. SNNs leverage temporal dynamics through spike-based, event-driven computation, allowing for more efficient processing of spatio-temporal event patterns compared to traditional ANNs [19]. When implemented on specialized neuromorphic hardware, SNNs can exploit their inherent sparsity, leading to significant gains in both latency and energy efficiency, directly addressing the challenges of conventional eye-tracking systems [20].

It is surprising that neuromorphic approaches have seen little use in wearable eye tracking, given their promise of inherent recurrence, improved latency and milliwatt power consumption. The *Retina* demon-

strated an SNN implementation with a pupil tracking error of 3.24px, power consumption between 2.89-4.8 mW, and latency of 5.57-8.01 ms [21]. This falls short of the accuracy performance of ANN decoders and its continuous resetting of neuron states may disrupt continuous tracking on neuromorphic hardware. Jiang et al. [22] presented an eye-tracking solution combining SNNs with event cameras that allows self-adjustment of time resolution with a maximum achievable resolution of 0.081 ms, but had a trade-off between spatial and temporal resolution.

This work introduces neuromorphic versions of top-performing AIS 2024 Challenge models (MambaPupil, CETM and BRAT) [23], replacing their recurrent and attention blocks with efficient LIF layers, and using depth-wise separable convolutions to require  $\sim 6\times$  fewer parameters and  $\sim 82\times$  fewer operations. Evaluated in continuous 1 kHz operations with 1 ms windows (Figure 1), the presented models achieve competitive accuracy on the 3ET+ dataset. This higher sampling rate was chosen to reflect the needs of vision scientists for high temporal resolution for precise sampling of saccades and micro-saccades [24,25]. Hardware projections demonstrate milliwatt-level power consumption and  $< 8$  ms latency, establishing a viable pathway for deploying complex eye-tracking on resource-constrained wearable devices. Our specific contributions include:

- We introduce a systematic method for converting recurrent and attention-based temporal modules from event-based ANNs into lightweight LIF layers, preserving temporal modelling capabilities at a fraction of the computational cost.
- We demonstrate that these neuromorphic models, evaluated in a continuous 1 kHz setting, achieve comparable performance with special-

- ized neuromorphic systems (i.e., Retina) while maintaining the flexibility of general-purpose ANN backbones.
- We achieve a  $30\text{-}1000\times$  reduction in theoretical compute and a  $22\text{-}45\times$  model size reduction, projecting sub-5 mW power consumption, thereby establishing a new operating point for high-speed, always-on pupil-tracking.

## II. RELATED WORKS

### A. Frame-based eye tracking

Traditional eye-tracking systems rely on frame-based cameras and are primarily built upon two methodological families, model-based and appearance-based approaches, which, while distinct, are frequently combined to improve robustness and accuracy.

1) *Model-based methods*: Model-based approaches extract geometric features (pupil center, corneal glints) and fit them to physiological eye models for gaze estimation [26,27]. While these methods can achieve high accuracy, they are notoriously sensitive to deployment conditions. Their performance is heavily dependent on consistent ambient lighting [28], high image resolution [29], and precise user-specific calibration [30]. Furthermore, they struggle with occlusions from eyelids and eyelashes, as well as deformations in eye shape [26].

2) *Appearance-based methods*: Appearance-based methods typically use convolutional neural networks (CNNs) for end-to-end regression from eye images to gaze points, offering robustness to shape and illumination variations. However, they demand large datasets, incur high computational costs, and are ultimately bounded by the frame rates and resolution of the input camera [31–35].

Both paradigms are constrained by physical camera limitations: standard high-speed cameras peak at 10–300 Hz, which is insufficient to accurately capture the fastest saccadic eye movements without motion blur. At the same time, kHz-rate cameras consume watts of power [29], exceeding mobile power budgets and motivating event-based alternatives.

### B. Event-based eye tracking

The asynchronous nature of event cameras enables microsecond temporal resolution, minimal motion blur, high dynamic range ( $>120$  dB), minimal latency and drastically lower power consumption [18], making them ideal for capturing rapid eye movements in power-constrained devices [14].

1) *Hybrid statistical methods*: Hybrid approaches combine event streams with occasional frames, using frames for model initialization and events for high-frequency updates. Angelopoulos et al.[6] achieved  $>10$  kHz with a parametric pupil model, but suffered from noise sensitivity and required recalibration. EV-EYE [36] achieved a tracking frequency of 38.4 kHz via pupil centroid tracking, but assumed fixed pupil shape between frames. Feng et al. [37] used software-emulated events and region of interest (ROI) prediction for efficiency, but operated at only 30 Hz.

These methods demonstrate high-frequency tracking potential but share limitations: complex data synchronization, computational overhead from fusion of event and frames, and persistent power consumption from frame-based components. These inherent limitations motivate exploring fully event-based approaches that eliminate the frame bottleneck entirely.

2) *Fully Event-based ANNs*: Fully event-based approaches process event streams directly using ANNs without frame-based sensors. However, ANNs require adapting sparse event data, typically by accumulating events into frame-like representations (e.g., voxel grids or kernel density estimates), which can introduce latency and sacrifice temporal resolution [22].

Representative methods include Li et al.’s [44] segmentation CNN with event-based ROI and E-Gaze’s [45] kernel density estimation with elliptical fitting. Other approaches such as Yang et al. [46] use events for frame interpolation before segmentation, further increasing computational burden.

Recurrent architectures have been explored to better model temporal dynamics, as the historical trajectory of the pupil provides valuable information for predicting its future location. Chen et al. proposed a sparse ConvLSTM that reduces operations by  $4.7\times$  compared to conventional CNNs [38], while Ryan et al. integrated gated recurrent units (GRUs) into YoloV3 for event-based tracking [47]. Recent innovations from the AIS 2024 Challenge [23] and its subsequent 2025 workshop [14] include state-space models like MambaPupil for selective temporal modeling [40] or the bidirectional transformer BRAT [43], see Table I. The state-of-the-art FACET framework demonstrates exceptional efficiency with 0.2 pixel error by directly regressing pupil parameters [29].

Despite these advances, most methods still rely on intermediate frame representations, limiting their temporal resolution and efficiency. Additional limitations include sensitivity to noise, special auxiliary hardware and dependency on synthetic training data, restricting real-world applicability.

Table I  
PERFORMANCE COMPARISON OF EYE-TRACKING MODELS ON 3ET+

Comparison of proposed SNN model variants with top-performing ANN models on the 2024 AIS Challenge [23] and of the 2025 event-based eye-tracking workshop [14]. ANN models achieve the strongest offline accuracy but rely on computationally heavy components (transformers, state-space blocks, attention) and have been evaluated at 20 Hz. The proposed SNN models operated in a continuous 1 kHz streaming paradigm and retain much of the ANN performance while reducing compute and parameter counts by orders of magnitude.  $\dagger$  denotes self-reported results on the evaluation set.

	Model	P1	P3	P5	P10	Euc. Dist.	Params	FLOPs
ANN	GTechVision [23]	4.16	31.70	61.08	92.26	4.94	410k	
	CB-ConvLSTM [38]			79.20	84.80	3.82	417k	1.09T
	PEPNet [39]	7.79	49.08	80.67	97.95	3.51	640k	459M
	GoSparse [23]	7.32	47.97	77.20	99.00	3.51	465k	
	MeMo [23]	6.53	50.87	89.36	99.05	3.20	5.4M	230M
	CETM [23]	23.91	83.83	96.31	99.26	2.03	7.1M	2.9G
	ERVT [23]	28.80	87.26	94.94	98.21	1.98	150k	157M
	MambaPupil [40]	33.75	90.73	97.05	99.42	1.67	8.59M	2.61T
	TDTracker [41]		91.20 $\dagger$	97.20 $\dagger$	99.20 $\dagger$	1.50	3.04M	265M
	BigBrain [42]	45.50	94.58	97.79	99.00	1.44	809k	110.4M
SNN	BRAT [43]			<b>97.80<math>\dagger</math></b>	<b>99.59<math>\dagger</math></b>	<b>1.14</b>	7.1M	5.8G
	Our (N=512)	9.59	54.76	79.10	96.25	3.66	352k	3.4M
	Our (N=256)	7.27	43.51	74.85	95.45	4.10	189k	3.1M
	Our (N=128)	8.57	48.80	77.27	95.85	3.90	<b>107k</b>	<b>2.9M</b>

3) *Fully Event-based Networks*: Fully neuromorphic approaches represent the most integrated solution, processing sparse event streams directly with SNNs to create a synergistic, event-driven pipeline. This paradigm eliminates the conversion to frames, leveraging the temporal dynamics of SNNs for efficient feature extraction and enabling lower latency and power consumption.

Key implementations demonstrate different strategies. Retina [21] achieved a 3.24px tracking error with  $<5$  mW and  $\sim 6$  ms latency on neuromorphic hardware. Jiang et al. [22] developed an SNN capable of self-adjusting its temporal resolution down to 0.081 ms, offering high adaptability but with a computationally intensive architecture. In contrast, Stoffregen et al. [48] pursued a model-based strategy, tracking corneal glints at 1 kHz, although this method is dependent on controlled illumination. Despite their promise, these systems reveal persistent trade-offs. SNN models face challenges with continuous tracking due to neuron state resets on hardware, while other approaches suffer from computational overhead or environmental dependencies. These limitations highlight the need for a robust and efficient neuromorphic solution, a gap the current work aims to address.

### III. METHODS

#### A. Data

The experiments in this work use the 3ET+ dataset, a benchmark for event-based eye tracking published as part of the AIS 2024 Event-based Eye Tracking

Challenge [23] and its subsequent 2025 iteration [14]. This dataset comprises real recordings from 13 participants, recorded in 2 to 6 sessions and captured using a DVXplorer Mini event camera [49]. During the recordings, subjects performed five distinct classes of eye activities: random movements, saccades, reading text, smooth pursuit, and blinks.

The dataset provides a real raw event stream. Each event is represented as a tuple  $(x_i, y_i, t_i, p_i)$ , where  $x_i$  and  $y_i$  are the spatial coordinates with a resolution of  $640 \times 480$  pixels,  $t_i$  is the timestamp with a temporal resolution of  $200 \mu\text{s}$ , and  $p_i$  is the polarity indicating the sign of the brightness change. The ground-truth annotations are provided at a frequency of 100 Hz. For each timestamp, the label consists of: 1) the spatial coordinates  $(x, y)$  of the pupil center, and 2) a binary value indicating whether the eye was blinking.

For the AIS 2024 Challenge [23], the primary evaluation metric on the Kaggle leaderboard was  $P$ -accuracy (specifically P10-accuracy). A prediction was considered correct if the Euclidean distance to the ground truth was within 10 pixels. Additional metrics, including  $P$ -accuracy for stricter tolerances ( $P = \{1, 3, 5\}$ ) and the  $L_2$  error, were also used for analysis. Notably, the 2025 iteration [14] updated its primary metric to mean pixel error (mean Euclidean distance) to better differentiate between high-performing models.

Table II  
PROPOSED NETWORK

The dimension of depthwise (DW) and pointwise (PW) convolution was chosen to match the dimensions used by CETM and MambaPupil. Convolutional layers have no bias and were padded to retain input dimensions. Hidden layers have fixed decay values that are initialized uniformly between 0.9 and 1. The output is the membrane potential of the final LIF layer with a learnable  $\beta$ , initialized to 0.9. Output channel  $N$  is a hyperparameter, with  $N \in (128, 256, 512)$ .

	Name	Dimensions	#Params
Conv1	DW Conv	$2 \times 2 \times 7 \times 7$	98
	IN, ReLU	2	
	PW Conv	$2 \times 32 \times 1 \times 1$	64
	IN, ReLU	32	
	Pool	$3 \times 3$	
Conv2	DW Conv	$32 \times 32 \times 5 \times 5$	800
	IN, ReLU	32	
	PW Conv	$32 \times 128 \times 1 \times 1$	4096
	IN, ReLU	128	
	Pool	$3 \times 3$	
Conv3	DW Conv	$128 \times 128 \times 5 \times 5$	3200
	IN, ReLU	128	
	PW Conv	$128 \times N \times 1 \times 1$	128N
	IN, ReLU	N	
	Pool	$4 \times 4$	
Flatten			
LIF1		$2N \times 256$	$512N + 256$
LIF2		$256 \times 64$	16,448
LIF3		$64 \times 2$	132
<b>Total</b>			$640N + 25,094$

### B. Implementation Details

All neuromorphic models were implemented using PyTorch [50] and snnTorch [19], with experiments conducted on a single NVIDIA L40S GPU. Raw events were discretized into 1 ms bins, matching the target 1 kHz inference frequency. Within each bin, polarities were aggregated and spatially downsampled to  $80 \times 60$  pixels to reduce computational load and match the effective resolution used in prior work.

Ground truth labels were upsampled from 100 Hz to 1 kHz using cubic B-spline interpolation to align with the event windows. This interpolation smooths the trajectory without introducing visible artifacts; visual inspection confirms sub-pixel deviations and avoids discontinuities between interpolation regions. Given the emphasis on low-power decoding rather than fine positional precision, this approximation is deemed acceptable with the benefit that it allows comparison to other reference solutions on the dataset.

To improve model robustness and prevent overfitting, the data was augmented during training. Spatial augmentations included horizontal and vertical flips and shifts. Temporal augmentations included tempo-

ral shifts and flips; in the latter case, polarities were inverted to maintain physical consistency. Additionally, we employed Event-Cutout [40], randomly masking spatio-temporal regions to encourage robustness.

Training used the Adam optimizer with a learning rate of  $1 \times 10^{-3}$ . The loss function combined position and velocity terms,  $L = L_{pos} + L_{vel}$ , where  $L_{pos}$  is the framewise MSE of pupil positions and  $L_{vel}$  is the MSE of first-order temporal differences. The velocity term encourages temporal smoothness and reduces jitter in high-frequency predictions.

Following the AIS 2024 protocol [23], blink periods were excluded from accuracy reporting. Model performance is reported using the standard train-validation-test paradigm, with 31 training, 9 validation and 11 testing sessions. Final results on the test set were reported for the epoch with peak validation performance. Models were trained on 450 ms sequences (450 timesteps with 1 ms bins) with a 1 ms stride across 40 epochs (Figure 1). While SNNs operate online at inference time, shorter windows proved detrimental during training. Due to the increased sparsity at 1 ms, many shorter sequences contain few events, forcing the network to infer gaze positions from empty frames. The 450 ms window increases the likelihood of multiple events bursts per sequence, improving convergence. This choice is consistent with top AIS performers [40,42] and is validated by our ablations in Table IV, which show that networks trained with shorter windows fail to learn.

For real-world assessment, models were evaluated in a continuous streaming mode: validation and test sessions were fed as uninterrupted streams of 1 ms windows without segmentation or overlap. During inference, the model uses no temporal context beyond the membrane potentials maintained by the leaky integrate-and-fire (LIF) neurons, making it suitable for 1 kHz real-time operation.

### C. Models

The proposed architecture adapts the convolutional backbone shared by MambaPupil [40], CETM, and BRAT [43], replacing their recurrent and attention modules with LIF layers. To reduce parameter count and computational load, all convolutional blocks are replaced with depth-wise separable convolutions (DSC), following the MobileNet design [53,54].

The proposed architecture comprises three convolutional blocks for spatial feature extraction. Each block follows the pattern: depth-wise (DW) convolution, instance normalization (IN), ReLU activation, pointwise (PW) convolution IN, ReLU, and average

Table III  
EFFICIENCY COMPARISON WITH RETINA

Efficiency comparison between our neuromorphic models and Retina. FLOPs include convolutional operations and LIF membrane updates. Sparse FLOPs reflect expected runtime cost given observed firing rates. Latency is projected according to the nature of neuromorphic execution, where each layer processes spikes in successive timesteps.<sup>1</sup> Sparse FLOPs use the dynamic firing rate from [21].<sup>2</sup> End-to-end on Synsense Speck [51].<sup>3</sup> Power is projected using the reported energy consumption for the effective arithmetic and memory operations of the neuromorphic chip SENECA [52].

Variant	Params	FLOPs	Sparse FLOPs	Power	Frequency	Latency
Retina [21]	63k	6.06M	$\approx 2.66M^1$	<5 mW <sup>2</sup>	$\leq 5$ kHz	>5 ms <sup>2</sup>
Our (N=512)	353k	3.4M	2.5M	4.9 mW <sup>3</sup>		
Our (N=256)	189k	3.1M	2.2M	4.2 mW <sup>3</sup>	1 kHz	
Our (N=128)	107k	2.9M	2M	3.9 mW <sup>3</sup>		3 ms

pooling. Instance normalization is used over Batch Normalization, due to its stability in streaming inference, where batch statistics are unavailable. The dimensions of each depth-wise separable block and the subsequent LIF layers are summarized in Table II.

The flattened convolutional features are passed into a stack of 3 dense LIF layers, replacing the original temporal modules. Hidden LIF layers use fixed decaying values sampled uniformly from  $\beta \sim U(0.9, 1)$ , providing a range of temporal decay constants and enabling multiple timescales of integration. The output LIF layer uses a learnable decay parameter, initialized to  $\beta_{out} = 0.9$ . The membrane potentials of the output LIF neurons, rather than their spike outputs, are used for regression. This produces continuous predictions while maintaining spike-based computation in hidden layers. Membrane potentials are initialized uniformly and reset by subtraction when thresholds are crossed. Although neuronal firing rates are not explicitly constrained, overall sparsity emerges naturally from the high input sparsity and LIF dynamics.

#### IV. EXPERIMENTAL RESULTS

##### A. Comparison with ANN-Based 3ET+ Models

Table I summarizes performance relative to the top ANN models from the Event-based Eye Tracking 2024 Challenge and the 2025 Workshop. These ANN architectures, ranging from state-space models (MambaPupil) to attention-driven designs (BRAT), achieve the strongest offline accuracy on 3ET+, but are typically trained at 100Hz and evaluated at 20Hz, and rely on computational mechanisms, such as, transformers, state-space blocks and attention, and do not scale to milliwatt-level or kHz-rate deployment.

The proposed spiking variants achieve 3.7-4.2px mean error across test sessions. This is 1-2px gap to the top ANN models (1.1 - 2.0px). This accuracy

drop is unsurprising given that heavy temporal modelling blocks are intentionally removed and replaced with lightweight neuromorphic layers. Despite this, the SNN variants preserve a substantial fraction of ANN performance while operating under drastically reduced computational budgets.

The efficiency advantages are shown in Figure 2. We observe a 20 $\times$  parameter reduction and 850 $\times$  floating point operations (FLOPs) reduction compared to CETM, the ANN variant most similar to the neuromorphic architectures proposed here. FLOP counts comprise convolutional operations as well as dense operations, membrane updates and decays in LIF layers. Even compared against more efficient ANN models (e.g. BigBrain) the neuromorphic variant reduces FLOPs by at least 30 $\times$  and 85% of the parameters. This reduction stems from three factors: (i) removal of attention and recurrence, (ii) depthwise-separable convolutions, and (iii) the sparsity and recurrence inherent to LIF neurons.

This architectural efficiency enables projected power consumption of 3.9-4.9 mW, calculated using the SENECA neuromorphic processor energy model [52] (1.4 pJ per arithmetic operation, 3.7 pJ per data load). The projected 3.9-4.9 mW range achieved by the neuromorphic models puts them on par with Retina (2.89-4.8 mW) [21] while maintaining continuous 1kHz inference. This is more than 50 $\times$  the temporal resolution of the operating frequency of the original ANN models.

Collectively, these results show that a substantial portion of ANN accuracy performance can be preserved under the constraints of neuromorphic systems, though ANNs remain superior where power and latency are not limiting factors. For wearable or embedded settings where power and latency are strict constraints, the SNN variants offer an attractive solution.

### B. Comparison with Neuromorphic Eye-Tracking Systems

Retina [21] represents the state-of-the-art for end-to-end neuromorphic eye tracking, providing a critical baseline for accuracy, power and latency on physical hardware. Retina is specifically engineered for energy efficiency, achieving 3.24px pupil tracking error on the INI-30 dataset, at measured power consumption of 2.89-4.8 mW and latency of 5.57-8.01 ms on the Synsense Speck neuromorphic processor [51].

A direct numerical comparison of accuracy is constrained by differences in evaluation datasets (INI-30 vs. 3ET+) and input resolution ( $64 \times 64$  vs.  $80 \times 60$ ). However, the SNN variants presented here achieve a comparable performance bracket of  $3.7\text{-}4.1\times$  on 3ET+, while hardware projections indicate a similar power envelope of 3.9-4.9 mW. This demonstrates that the presented approach, converting high-performance ANN backbones, can reach the same critical accuracy-efficiency trade-off as a model like Retina, which was designed from the ground up.

The key distinction lies in architectural philosophy and demonstrated flexibility. Retina employs a highly specialized, shallow convolutional SNN front-end paired with a fixed, non-spiking temporal weighted-sum filter, a design tightly coupled to the constraints of its target hardware (Speck). In contrast, the work presented here demonstrates a modular conversion pathway. By systematically replacing recurrent and attention blocks in top-performing ANNs (e.g., MambaPupil, CETM) with LIF layers, complex temporal modelling can be efficiently offloaded to an SNN’s inherent dynamics without hardware-specific architectural specialization. This provides a more generalizable blueprint for migrating other event-based vision architectures to the neuromorphic domain.

Latency is projected according to the nature of neuromorphic execution, where each consecutive spiking layers is processed subsequently. Given Retina’s 8 layers and a measured latency of 5.57-8.01 ms, this projection is conservative. The proposed model’s pipelined architecture, with three successive LIF layers, yields a theoretical latency of 3 ms, which is lower than Retina’s measured latency. It is crucial to note that this is a projection, whereas Retina’s figure is a hardware measurement; end-to-end deployment is required for a definitive comparison. Nevertheless, this neuromorphic architecture is inherently suited for continuous, real-time tracking of saccadic movements.

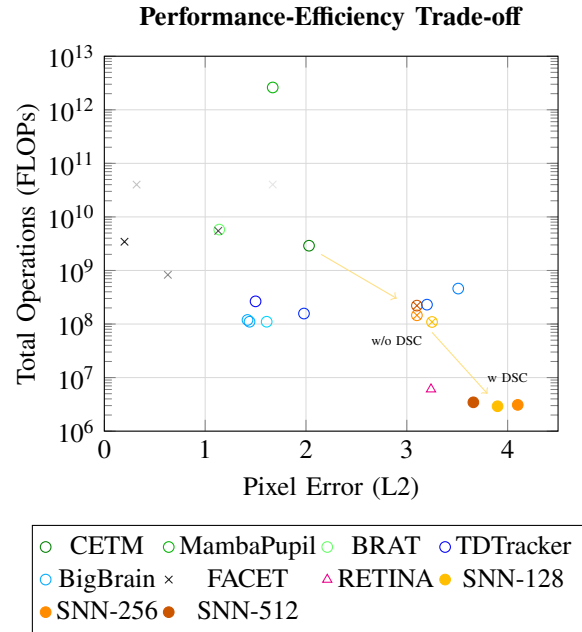


Figure 2. Pixel error is shown against total FLOPs on a log scale. Circles denote models trained on 3ET+, crosses on EV-Eye, and triangles on INI-30. Performance is taken from [14,23], [29] and [21], respectively. Notably, 3ET+ uses a spatial resolution of  $80 \times 60$  compared to  $64 \times 64$  of EV-Eye and INI-30. Our spiking variants (solid circles) retain acceptable accuracies while operating at orders-of-magnitude lower compute. These models reach similar efficiency as Retina while offering greater architectural flexibility. Ideal models lie toward the lower-left corner (low error, low compute).

## V. DISCUSSION

This work demonstrates that spiking neural networks can achieve the critical balance needed for real-time eye tracking in wearable systems: viable accuracy with extreme efficiency. By converting recurrent ANN architectures into lightweight, LIF-based SNNs, we reduce computational demands by three orders of magnitude, while maintaining acceptable performance on the 3ET+ benchmark. Specifically, we reduce computational costs by a factor of 30-1000 $\times$  and compress model size by 22-44 $\times$ , all while sustaining an accuracy of 3.7-4.1px. Crucially, the evaluation, conducted in continuous 1 kHz operation with architecture-based power projections, confirms that these models are deployable on neuromorphic hardware for wearable eye tracking systems where milliwatt-level power consumption is advantageous.

The performance comparison reveals fundamentally different design priorities between ANN and neuromorphic approaches. While ANNs can achieve superior offline accuracy when evaluated at 20 Hz

sampling rate, they often rely on hardware that is too power-hungry or bulky for wearable eye trackers. In contrast, the presented neuromorphic approach focuses on efficient, continuous 1 kHz tracking within stringent power budgets. This enables the capture of fine-grained eye dynamics, such as micro-saccades, with the high temporal and spatial accuracy needed for user authentication or evaluating attention. This trade-off underscores a limitation in conventional benchmarks, that prioritize offline accuracy without accounting for the operational constraints of always-on wearable devices.

Table IV  
ABLATION STUDY RESULTS

Impact of architectural and training choices on model performance on the validation set. Notably, there are significant performance differences to the testing set.

Variant	P5	P10	Euc. Dist.	Params	FLOP
<i>Benchmark</i>	64.20	87.49	5.26	<b>352k</b>	<b>3.4M</b>
<b>Convolution - Depth-wise Separable Convolution (DSC)</b>					
w/o DSC-512	<b>75.70</b>	<b>92.01</b>	<b>4.24</b>	2M	280M
w/o DSC-256	74.19	91.36	4.44	1.1M	203M
w/o DSC-128	74.36	90.77	4.44	598k	164M
<b>Window - 450</b>					
→ 150	61.18	84.89	5.29	<i>unchanged</i>	
<b>Stride - 1</b>					
→ 10	52.27	86.20	6.07	<i>unchanged</i>	
→ 50	42.04	76.52	7.65	<i>unchanged</i>	
<b>Loss - Velocity Loss</b>					
→ Spatial					
MSE	59.74	84.75	5.72	<i>unchanged</i>	

Beyond raw efficiency, the temporal dynamics inherent to LIF neurons provide distinct advantages for processing event-based data streams. Unlike ANNs, SNNs naturally maintain state across timesteps, offering built-in smoothing and noise suppression without requiring explicit architectural mechanisms for temporal modeling. This makes them particularly suited for continuous sensor data where timing precision and energy efficiency are critical. These properties make SNNs highly suited for real-time eye tracking, as demonstrated by the comparable performance between the presented approach and the specialized Retina neuromorphic benchmark.

Looking forward, closing the accuracy gap with state-of-the-art ANNs will require addressing of the fundamental benchmark mismatches between offline evaluation and real-time operation. Future work should pursue three key directions; First, end-to-end deployment and optimization on neuromorphic

hardware is essential to validate power and latency projections and identify potential bottlenecks in real-world operation. Second, other high-performance architectures such as BigBrain and FACET could be adapted to neuromorphic systems, which could potentially achieve better accuracy while maintaining efficiency. Finally, incorporating temporal filtering mechanisms similar to Retina’s weighted-sum approach could enhance prediction stability and smoothness, particularly given the strong performance improvements demonstrated in their work. These combined approaches, hardware validation, architectural expansion, and temporal refinement, represent promising pathways for advancing neuromorphic eye tracking toward both high accuracy and extreme efficiency.

## VI. CONCLUSION

This work demonstrates that event-based eye-tracking architectures can be effectively redesigned as spiking neural networks, achieving significant efficiency gains while maintaining practical accuracy for real-time wearable use. By replacing the recurrent and attention components of high-performing ANN backbones with lightweight LIF layers, we reduce computational cost by 30-1000× and compress model size 22-45×, while sustaining 3.7-4.1px error on the 3ET+ benchmark. Using the SENeCA neuromorphic energy model, our most efficient variants operate at an estimated 3.9-4.9 mW with ≈3 ms latency at 1 kHz, making them suitable for continuous, always-on eye tracking systems with a tight power and latency constraints. Although an accuracy gap remains relative to the leading ANN models, the presented results show that neuromorphic redesign can preserve much of their performance at a fraction of the computational footprint. Overall, this work provides a concrete step toward deployable, low-power, event-driven gaze estimation. It’s hoped that the presented findings hope that our findings, and the accompanying open-source implementations, encourage further exploration of neuromorphic architectures for high-speed, energy-constrained eye-tracking systems.

## VII. FUNDING

This research was supported through the NimbleAI project, funded via the Horizon Europe Research and Innovation programme (Grant Agreement 101070679), and UKRI under the UK government’s Horizon Europe funding guarantee (Grant Agreement 10039070); the Horizon Europe AIDA4Edge project (Grant Agreement 101160293); and the EPSRC Edgy Organism project (EP/Y030133/1).

## REFERENCES

[1] F. Kano, Y. Kawaguchi, and Y. Hanling, “Experimental evidence that uniformly white sclera enhances the visibility of eye-gaze direction in humans and chimpanzees,” *Elife*, vol. 11, p. e74086, 2022.

[2] S. Wacewicz, J. O. Perea-García, Z. Lewandowski, and D. P. Danel, “The adaptive significance of human scleral brightness: an experimental study,” *Scientific reports*, vol. 12, no. 1, p. 20261, 2022.

[3] R. J. Leigh and D. S. Zee, *The neurology of eye movements*. Oxford university press, 2015.

[4] K. Harezlak and P. Kasprowski, “Application of eye tracking in medicine: A survey, research issues and challenges,” *Computerized Medical Imaging and Graphics*, vol. 65, pp. 176–190, 2018.

[5] J. Moreno-Arjonilla, A. López-Ruiz, J. R. Jiménez-Pérez, J. E. Callejas-Aguilera, and J. M. Jurado, “Eye-tracking on virtual reality: a survey,” *Virtual Real.*, vol. 28, no. 1, Mar. 2024.

[6] A. N. Angelopoulos, J. N. Martel, A. P. Kohli, J. Conradt, and G. Wetzstein, “Event based, near eye gaze tracking beyond 10,000 hz,” *arXiv preprint arXiv:2004.03577*, 2020.

[7] A. Fischer-Janzen, T. M. Wendt, and K. Van Laerhoven, “A scoping review of gaze and eye tracking-based control methods for assistive robotic arms,” *Front. Robot. AI*, vol. 11, p. 1326670, Feb. 2024.

[8] J. Xia, W. Qu, W. Huang, J. Zhang, X. Wang, and M. Xu, “Sparse local patch transformer for robust face alignment and landmarks inherent relation learning,” in *2022 IEEE/CVF Conference on Computer Vision and Pattern Recognition (CVPR)*, 2022, pp. 4042–4051.

[9] X. Fan, F. Wang, D. Song, Y. Lu, and J. Liu, “GazMon: Eye gazing enabled driving behavior monitoring and prediction,” *IEEE Trans. Mob. Comput.*, vol. 20, no. 4, pp. 1420–1433, Apr. 2021.

[10] A. T. Bahill, M. R. Clark, and L. Stark, “Glissades—eye movements generated by mismatched components of the saccadic motoneuronal control signal,” *Mathematical Biosciences*, vol. 26, no. 3-4, pp. 303–318, 1975.

[11] R. A. Abrams, D. E. Meyer, and S. Kornblum, “Speed and accuracy of saccadic eye movements: characteristics of impulse variability in the oculomotor system,” *Journal of Experimental Psychology: Human Perception and Performance*, vol. 15, no. 3, p. 529, 1989.

[12] K. Rayner, “Eye movements and attention in reading, scene perception, and visual search,” *The quarterly journal of experimental psychology*, vol. 62, no. 8, pp. 1457–1506, 2009.

[13] M. L. Mele and S. Federici, “Gaze and eye-tracking solutions for psychological research,” *Cognitive processing*, vol. 13, no. Suppl 1, pp. 261–265, 2012.

[14] Q. Chen, C. Gao, M. Liu, D. Perrone, Y. R. Pei, Z. Wang, Z. Zou, S. Tan, T. Han, G. Lu *et al.*, “Event-based eye tracking: 2025 event-based vision workshop,” in *2025 IEEE/CVF Conference on Computer Vision and Pattern Recognition Workshops (CVPRW)*. IEEE, 2025, pp. 5164–5176.

[15] P. Lichtsteiner, C. Posch, and T. Delbrück, “A  $128 \times 128$  120 db  $15\mu s$  latency asynchronous temporal contrast vision sensor,” *IEEE journal of solid-state circuits*, vol. 43, no. 2, pp. 566–576, 2008.

[16] K. Iddrisu, W. Shariff, P. Corcoran, N. E. O’Connor, J. Lemley, and S. Little, “Event camera-based eye motion analysis: A survey,” *IEEE Access*, vol. 12, pp. 136 783–136 804, 2024.

[17] G. Taverni, D. Paul Moeyns, C. Li, C. Cavaco, V. Motsnyi, D. San Segundo Bello, and T. Delbrück, “Front and back illuminated dynamic and active pixel vision sensors comparison,” *IEEE Transactions on Circuits and Systems II: Express Briefs*, vol. 65, no. 5, pp. 677–681, 2018.

[18] G. Gallego, T. Delbrück, G. Orchard, C. Bartolozzi, B. Taba, A. Censi, S. Leutenegger, A. J. Davison, J. Conradt, K. Daniilidis *et al.*, “Event-based vision: A survey,” *IEEE transactions on pattern analysis and machine intelligence*, vol. 44, no. 1, pp. 154–180, 2020.

[19] J. K. Eshraghian, M. Ward, E. O. Neftci, X. Wang, G. Lenz, G. Dwivedi, M. Bennamoun, D. S. Jeong, and W. D. Lu, “Training spiking neural networks using lessons from deep learning,” *Proceedings of the IEEE*, vol. 111, no. 9, pp. 1016–1054, 2023.

[20] M. Davies, A. Wild, G. Orchard, Y. Sandamirskaya, G. A. F. Guerra, P. Joshi, P. Plank, and S. R. Risbud, “Advancing neuromorphic computing with loihi: A survey of results and outlook,” *Proceedings of the IEEE*, vol. 109, no. 5, pp. 911–934, 2021.

[21] P. Bonazzi, S. Bian, G. Lippolis, Y. Li, S. Sheik, and M. Magno, “Retina: Low-power eye tracking with event camera and spiking hardware. ieee,” in *CVF Conference on Computer Vision and Pattern Recognition (CVPR) Workshops*, vol. 1, 2024.

[22] Y. Jiang, W. Wang, L. Yu, and C. He, “Eye tracking based on event camera and spiking neural network,” *Electronics*, vol. 13, no. 14, p. 2879, 2024.

[23] Z. Wang, C. Gao, Z. Wu, M. V. Conde, R. Timofte, S.-C. Liu, Q. Chen, Z.-j. Zha, W. Zhai, H. Han *et al.*, “Event-based eye tracking. ais 2024 challenge survey,” in *Proceedings of the IEEE/CVF Conference on Computer Vision and Pattern Recognition*, 2024, pp. 5810–5825.

[24] M. H. Raju, S. Aziz, M. J. Proulx, and O. Komogortsev, “Evaluating eye tracking signal quality with real-time gaze interaction simulation: A study using an offline dataset,” in *Proceedings of the 2025 Symposium on Eye Tracking Research and Applications*, 2025, pp. 1–11.

[25] B. Angele, Z. Gunes Ozkan, M. Serrano-Carot, and J. A. Dufnabeitia, “How low can you go? tracking eye movements during reading at different sampling rates,” *Behavior Research Methods*, vol. 57, no. 7, p. 195, 2025.

[26] C. Mestre, J. Gautier, and J. Pujol, “Robust eye tracking based on multiple corneal reflections for clinical applications,” *Journal of biomedical optics*, vol. 23, no. 3, pp. 035 001–035 001, 2018.

[27] C.-C. Lai, S.-W. Shih, and Y.-P. Hung, “Hybrid method for 3-d gaze tracking using glint and contour features,” *IEEE Transactions on Circuits and Systems for Video Technology*, vol. 25, no. 1, pp. 24–37, 2015.

[28] A. Gibaldi, M. Vanegas, P. J. Bex, and G. Maiello, “Evaluation of the tobii eyex eye tracking controller and matlab toolkit for research,” *Behavior research methods*, vol. 49, no. 3, pp. 923–946, 2017.

[29] J. Ding, Z. Wang, C. Gao, M. Liu, and Q. Chen, “Facet: Fast and accurate event-based eye tracking using ellipse modeling for extended reality,” in *2025 IEEE International Conference on Robotics and Automation (ICRA)*. IEEE, 2025, pp. 10 347–10 354.

[30] D. Geisler, D. Fox, and E. Kasneci, “Real-time 3d glint detection in remote eye tracking based on bayesian inference,” in *2018 IEEE International Conference on Robotics and Automation (ICRA)*. IEEE, 2018, pp. 7119–7126.

[31] X. Zhang, Y. Sugano, M. Fritz, and A. Bulling, “Mpigaze: Real-world dataset and deep appearance-based gaze estimation,” *IEEE transactions on pattern analysis and machine intelligence*, vol. 41, no. 1, pp. 162–175, 2017.

[32] P. L. Mazzeo, D. D’Amico, P. Spagnolo, and C. Distante, “Deep learning based eye gaze estimation and prediction,” in *2021 6th International Conference on Smart and Sustainable Technologies (SpliTech)*. IEEE, 2021, pp. 1–6.

[33] K. I. Lee, J. H. Jeon, and B. C. Song, “Deep learning-based pupil center detection for fast and accurate eye track-

ing system,” in *European Conference on Computer Vision*. Springer, 2020, pp. 36–52.

[34] O. Deane, E. Toth, and S.-H. Yeo, “Deep-saga: a deep-learning-based system for automatic gaze annotation from eye-tracking data,” *Behavior Research Methods*, vol. 55, no. 3, pp. 1372–1391, 2023.

[35] J. Kim, M. Stengel, A. Majercik, S. De Mello, D. Dunn, S. Laine, M. McGuire, and D. Luebke, “Nvgaze: An anatomically-informed dataset for low-latency, near-eye gaze estimation,” in *Proceedings of the 2019 CHI conference on human factors in computing systems*, 2019, pp. 1–12.

[36] G. Zhao, Y. Yang, J. Liu, N. Chen, Y. Shen, H. Wen, and G. Lan, “Ev-eye: Rethinking high-frequency eye tracking through the lenses of event cameras,” *Advances in Neural Information Processing Systems*, vol. 36, pp. 62 169–62 182, 2023.

[37] Y. Feng, N. Goulding-Hotta, A. Khan, H. Reyserhove, and Y. Zhu, “Real-time gaze tracking with event-driven eye segmentation,” in *2022 IEEE Conference on Virtual Reality and 3D User Interfaces (VR)*. IEEE, 2022, pp. 399–408.

[38] Q. Chen, Z. Wang, S.-C. Liu, and C. Gao, “3ET: Efficient Event-based Eye Tracking using a Change-Based ConvLSTM Network,” in *2023 IEEE Biomedical Circuits and Systems Conference (BioCAS)*, Oct. 2023, pp. 1–5, arXiv:2308.11771 [cs]. [Online]. Available: <http://arxiv.org/abs/2308.11771>

[39] H. Ren, J. Zhu, Y. Zhou, H. Fu, Y. Huang, and B. Cheng, “A simple and effective point-based network for event camera 6-dofs pose relocalization,” in *Proceedings of the IEEE/CVF Conference on Computer Vision and Pattern Recognition*, 2024, pp. 18 112–18 121.

[40] Z. Wang, Z. Wan, H. Han, B. Liao, Y. Wu, W. Zhai, Y. Cao, and Z.-J. Zha, “Mambapupil: Bidirectional selective recurrent model for event-based eye tracking,” in *Proceedings of the IEEE/CVF Conference on Computer Vision and Pattern Recognition*, 2024, pp. 5762–5770.

[41] H. Ren, X. Lin, H. Huang, Y. Zhou, and B. Cheng, “Exploring temporal dynamics in event-based eye tracker,” *arXiv preprint arXiv:2503.23725*, 2025.

[42] Y. R. Pei, S. Brüters, S. Crouzet, D. McLelland, and O. Coenen, “A lightweight spatiotemporal network for online eye tracking with event camera,” in *Proceedings of the IEEE/CVF Conference on Computer Vision and Pattern Recognition*, 2024, pp. 5780–5788.

[43] Y. Wu, H. Han, J. Chen, W. Zhai, Y. Cao, and Z.-j. Zha, “Brat: Bidirectional relative positional attention transformer for event-based eye tracking,” in *Proceedings of the Computer Vision and Pattern Recognition Conference*, 2025, pp. 5136–5144.

[44] N. Li, A. Bhat, and A. Raychowdhury, “E-track: Eye tracking with event camera for extended reality (xr) applications,” in *2023 IEEE 5th International Conference on Artificial Intelligence Circuits and Systems (AICAS)*, 2023, pp. 1–5.

[45] N. Li, M. Chang, and A. Raychowdhury, “E-gaze: Gaze estimation with event camera,” *IEEE Transactions on Pattern Analysis and Machine Intelligence*, vol. 46, no. 7, pp. 4796–4811, 2024.

[46] Y. Yang, G. Zhao, and Y. Shen, “High frequency event-based eye tracking towards mental health diagnosis,” in *2023 IEEE International Symposium on Mixed and Augmented Reality Adjunct (ISMAR-Adjunct)*. IEEE, 2023, pp. 335–339.

[47] C. Ryan, B. O’Sullivan, A. Elrasad, A. Cahill, J. Lemley, P. Kiely, C. Posch, and E. Perot, “Real-time face & eye tracking and blink detection using event cameras,” *Neural Networks*, vol. 141, pp. 87–97, 2021.

[48] T. Stoffregen, H. Daraei, C. Robinson, and A. Fix, “Event-based kilohertz eye tracking using coded differential lighting,” in *Proceedings of the IEEE/CVF Winter Conference on Applications of Computer Vision*, 2022, pp. 2515–2523.

[49] *DVXplorer Mini*, Specifications, Inivation, Nov. 2025. [Online]. Available: [https://docs.inivation.com/\\_static/hardware\\_guides/dvxplorer-mini.pdf](https://docs.inivation.com/_static/hardware_guides/dvxplorer-mini.pdf)

[50] A. Paszke, S. Gross, F. Massa, A. Lerer, J. Bradbury, G. Chanan, T. Killeen, Z. Lin, N. Gimelshein, L. Antiga, A. Desmaison, A. Kopf, E. Z. Yang, Z. DeVito, M. Raison, A. Tejani, S. Chilamkurthy, B. Steiner, L. Fang, J. Bai, and S. Chintala, “Pytorch: An imperative style, high-performance deep learning library,” *CoRR*, vol. abs/1912.01703, 2019. [Online]. Available: <http://arxiv.org/abs/1912.01703>

[51] M. Yao, O. Richter, G. Zhao, N. Qiao, Y. Xing, D. Wang, T. Hu, W. Fang, T. Demirci, M. De Marchi *et al.*, “Spikes-based dynamic computing with asynchronous sensing-computing neuromorphic chip,” *Nature Communications*, vol. 15, no. 1, p. 4464, 2024.

[52] G. Tang, A. Safa, K. Shidqi, P. Detterer, S. Traferro, M. Koni-jnenburg, M. Sifalakis, G.-J. van Schaik, and A. Yousefzadeh, “Open the box of digital neuromorphic processor: Towards effective algorithm-hardware co-design,” in *2023 IEEE International Symposium on Circuits and Systems (ISCAS)*. IEEE, 2023, pp. 1–5.

[53] L. Sifre and S. Mallat, “Rigid-motion scattering for texture classification,” *arXiv preprint arXiv:1403.1687*, 2014.

[54] A. G. Howard, M. Zhu, B. Chen, D. Kalenichenko, W. Wang, T. Weyand, M. Andreetto, and H. Adam, “Mobilennets: Efficient convolutional neural networks for mobile vision applications,” *arXiv preprint arXiv:1704.04861*, 2017.